Surface Science 613 (2013) 6–14

Contents lists available at SciVerse ScienceDirect

Surface Science

journal homepage: www.elsevier.com/locate/susc

Surface Science Prospectives

# Covalently bonded networks through surface-confined polymerization

Mohamed El Garah [a,*], Jennifer M. MacLeod [a], Federico Rosei [a,b]

[a] Centre Énergie, Matériaux et Télécommunication, Institut National de la Recherche Scientifique, Université du Québec, 1650 boulevard Lionel-Boulet, Varennes, QC, J3X 1S2, Canada
[b] Center for Self-Assembled Chemical Structures, McGill University, H3A 2K6, Montreal, QC, Canada

ARTICLE INFO

*Article history:*
Received 31 January 2013
Accepted 15 March 2013
Available online 26 March 2013

*Keywords:*
Polymerization
STM
Dehalogenation
Ullmann coupling
Surface

ABSTRACT

The prospect of synthesizing ordered, covalently bonded structures directly on a surface has recently attracted considerable attention due to its fundamental interest and for potential applications in electronics and photonics. This prospective article focuses on efforts to synthesize and characterize epitaxial one- and two-dimensional (1D and 2D, respectively) polymeric networks on single crystal surfaces. Recent studies, mostly performed using scanning tunneling microscopy (STM), demonstrate the ability to induce polymerization based on Ullmann coupling, thermal dehalogenation and dehydration reactions. The 2D polymer networks synthesized to date have exhibited structural limitations and have been shown to form only small domains on the surface. We discuss different approaches to control 1D and 2D polymerization, with particular emphasis on the surface phenomena that are critical to the formation of larger ordered domains.



## 1. Introduction

Molecular self-assembly is a fundamental process that can be harnessed for a variety of nanotechnology applications. The study of molecular epitaxial growth at surfaces may provide critical new insight for their integration in molecular electronics [1–3]. Various self-assembled structures held together by non-covalent bonds have been achieved based on different intermolecular interactions such as hydrogen bonds [4–9], van der Waals interaction [10], halogen bonds [11–13] and metal–organic coordination [14–16]. These types of interactions, which have the advantage of the reversibility of bonding on the surface, offer an opportunity for forming long range ordered structures in two dimensions. However, self-assembly does have some limitations, most notably that the intermolecular interaction is relatively weak and therefore leads to fragile structures. This challenge can be overcome by forming covalent bonds between molecules [17,18]. Various studies have been performed with the objective of creating macromolecular structures on a surface starting from small building blocks [19,20]. A major advantage provided by covalent bonding, in addition to the mechanical rigidity of the structures, is the effective charge transport through the bond [21]. Conjugated polymers are ubiquitous semiconducting materials that are increasingly used in applications. Their integrated optoelectronic properties make them well-suited for use as active components in electronic devices [3,21,22], such as photovoltaic cells [23], organic light-emitting diodes [24–26] and organic field-effect transistors [27–29]. 1D or 2D conjugated polymer nanostructures, in which covalent bonds provide robust structural and thermal properties, are increasingly being synthesized using a bottom-up approach where monomers are deposited onto a surface and subsequently made to react. To date, such surface confined polymers have been synthesized using various routes including Ullmann dehalogenation [30,31], thermal cleaving of carbon-halide bonds [19,32,33] and dehydration reactions [34–38]. Although 1D polymer "lines" can be synthesized with reasonably high quality, 2D networks have so far exhibited small domains and a high defect density. Thus, the search for improved pathways to synthesize large covalently bonded 2D nanostructures with low defect densities is intensifying, as is the effort to probe and subsequently optimize their electronic properties.

The role of the substrate, specifically its orientation and chemical properties, in the polymerization process cannot be overemphasized. Depending on the synthesis approach employed, the surface can be used as both a catalyst and/or a template to confine the polymerization reaction. The resulting polymeric structures have been characterized using standard surface science techniques including STM and X-ray photoemission spectroscopy (XPS), complimented with density functional theory (DFT) calculations [20,30,35,39]. These characterization techniques provide information about both structural and electronic properties, critical for understanding and controlling the polymerization reaction on the surface [3,40–42].

In this prospective we describe recent work on 1D and 2D surface-confined polymerization reactions and discuss the surface phenomena that may play a key role in addressing the current limitations of polymerization reactions, particularly in two dimensions. These include the reactivity of monomers on the surface, the role of diffusion in the spatial extension of the network and the optimization of reaction intermediates.

* Corresponding author at: Centre Énergie, Matériaux et Télécommunication, Institut National de la Recherche Scientifique, Université du Québec, 1650 boulevard Lionel-Boulet, Varennes, QC J3X 1S2, Canada. Tel.: +15142286986.
*E-mail address:* rosei@emt.inrs.ca (F. Rosei).

0039-6028/$ – see front matter © 2013 Elsevier B.V. All rights reserved.
http://dx.doi.org/10.1016/j.susc.2013.03.015

## 2. One-dimensional surface-confined polymerization

The simplest geometric examples of surface-confined growth of conjugated polymers have been demonstrated through the creation of 1D lines of polydiacetylene [43] and polyphenylene [30]. These structures were achieved using different chemical routes: photochemical activation, voltage pulsing with an STM tip and Ullmann coupling, respectively, and are discussed in more detail hereafter.

### 2.1. Diacetylene polymerization

Grim et al. first reported the photo-polymerization of diacetylene molecules on HOPG at the solution/solid interface [43]. The reactants and products of the polymerization reaction were characterized, with submolecular resolution, by STM. The structure adopted by the diacetylene-containing isophtalic acid (ISA) on HOPG comprises adjacent lamellae of diacetylene. Following irradiation with ultraviolet light (UV), a contrast change within the structure was observed, which was attributed to the polymerization of the diacetylene molecules. This interpretation was then confirmed by measuring the intermolecular spacing, which was found to expand from 9.44 ± 0.09 Å to 9.81 ± 0.05 Å, measured as the spacing between two adjacent ISA groups in the structure.

Okawa and Aono subsequently reported the creation of polymer nanowires through a polymerization chain reaction in diacetylene molecules initiated by applying a voltage pulse with the STM tip [44,45]. Two monomers, 10,12-pentacosadiynoic acid and 10,12-nonacosadiynoic acid, were self-assembled and made to react on the HOPG substrate. The authors demonstrated the ability to control the initiation and termination of the chain polymerization of the 10,12 pentacosadiynoic acid monomer [44]. This control was attained through the creation of a defect hole in the HOPG using the STM tip; the hole then acted as a topological termination site for the polymerization reaction [46]. The dependence of the polymerization probability with the duration of the applied voltage pulse was reported by Sullivan et al. [47]. They correlated increasing polymerization probability with increasing time of the voltage pulse. In addition, they suggested that pit edges terminate the polymerization reaction because topochemical conditions are interrupted at such a site. A similar effect was reported by Okawa and Aono, where the domains boundaries were found to interrupt the polymerization reaction [45].

### 2.2. Polythiophene

Using the electrochemical epitaxial polymerization (ECEP) technique [48], based on step-by-step electro-polymerization of monomers using a voltage pulse, Sakaguchi et al. demonstrated the formation of linear polythiophene wires up to 75 nm in length on the surface of an iodine-terminated Au(111) electrode [48,49]. The polymers were formed after the Au(111) electrode was introduced into a cell containing both iodine and 3-butoxy-4-methylthiophene (BuOMT) monomers and a step-function voltage pulse was applied. By using the ECEP technique in a solution containing different-types of monomers, the authors demonstrated the formation of polythiophene chains as diblocks, triblocks and multiblocks [49]. The structures of these polymers were reproduced using a second method, in which the I-Au(111) electrode was moved between two cells that each contained a single monomer species (3-octyloxy-4-methylthiophene (C8OMT) or 3-octyl-4-methylthiophene (C8MT)). In both cases, the authors differentiated the blocks using the contrast of the structures in STM images; the polythiophenes formed from C8OMT appear bright and solid whereas the C8MT appear as discrete elements.

### 2.3. 1D Ullmann-coupled structures

The success of the ECEP method, which is predicated on the presence of the Au(111) surface as electrode, stimulated interest in identifying other methods for on-surface polymerization. Ullmann coupling, a reaction based on catalyzed dehalogenation, was identified more than 100 years ago [50]. More recently, each of the Ullmann reaction steps was achieved using an STM tip on Cu(111) [51], when Hla et al. reported the synthesis of biphenyls from iodobenzene molecules in three steps. First, tunneling electrons from the STM tip were used to induce the dissociation of iodobenzene to iodine and phenyl. Second, the STM tip was used to move two phenyls close to one other. Finally, conjugated coupling was accomplished through application of a voltage pulse.

Lipton-Duffin et al. also translated Ullmann polymerization to a single crystal copper surface [30], leading to the formation of two different polyphenylenes: *meta*-polyphenlene (PMP) and *para*-polyphenylene (PPP). PPP and PMP were synthesized on the Cu(110) surface, under UHV conditions, by Ullmann dehalogenation from 1,4 diiodobenzene (*para*-dIB) and 1,3 diiodobenzene (*meta*-dIB) precursors, respectively [30]. These results clearly illustrate that the geometry of the polymerized structures is dependent on the position of the halogen substituent on the molecule. The PPP chains represent the end result of polymerizing *para*-dIB monomers by annealing at 500 K for 5–10 min. In STM images, the PPP chains appear as discrete elements oriented along $[1\ \ 1\ \ 0]$ and separated laterally by lines of iodine atoms (Fig. 1a). The periodicity of PPP was measured at 4.1 Å (profile on Fig. 1a). Approximately the same value was found between two covalently bonded phenyls in the gas phase using DFT calculations (SI of reference [30]). Thus, the adsorption of *para*-dIB on Cu(110) followed by annealing at 500 K led to the formation of aligned polymer chains.

On the other hand, the polymerization of *meta*-dIB on Cu(110) produced two structures: zigzag lines and macrocycles (Fig. 1b). The formation of the zigzag polymer chains can be explained by the presence of kinks introduced by the symmetry of the *meta*-dIB monomers [30]. In addition to PMP, circular macrocycles were found on the surface as shown in the inset of Fig. 1c. Both pentagonal and hexagonal structures were identified.

Lipton-Duffin et al. later reported the formation of ordered poly (3,4-ethylenedioxythiophene) (PEDOT) chains directly on the Cu(110) surface, which was again used as both a template and a catalyst [31]. Different structures like monomers, dimers and trimers were observed on the surface (Fig. 2a) following the deposition of 2,5-diiodo 3,4-ethylenedioxythiophene) (DIEDOT). These structures are surrounded by regions with c($2 \times 2$) symmetry, ascribed to iodine atoms adsorbed on hollow sites of the Cu(110) surface [31], confirming the dehalogenation of the molecules. In combination with DFT calculations, the experimental results show that the dehalogenated molecules reside above the long bridge sites of Cu(110), oriented with the sulfur atoms pointing toward the surface. Three interactions stabilize the EDOT elements: C – Cu, Cu – S bonds with the surface and the van der Waals interaction between adjacent molecules.

Increasing the DIEDOT coverage led to the formation of bonded lines formed from dimeric and trimeric structures (Fig. 2a). These structures appear as discrete elements in $[1\ \ 1\ \ 0]$ and a continuous element in [001]. Surfaces saturated by DIEDOT show the formation of PEDOT oligomers and I-c($2 \times 2$) structures (supporting information of reference [31]). The oligomer chains are the result of an extended polymerization reaction between EDOT monomers along the [001] direction (supporting information in reference [31]). It was thus shown that the strong molecule-surface interaction dictates the formation of the cis configuration of the polymer chains. This occurrence was surprising and unexpected, since in the gas phase only the trans configuration is present.

Identifying the intermediate state of the Ullmann coupling reaction on the surface is a crucial step to understanding the mechanism of the reaction. McCarty and Weiss proposed that the radicals, in an intermediate state, are linked by molecule-molecule and surface-mediated interactions [52,53]. Lipton-Duffin et al. and Walch et al. proposed that the copper atoms link two adjacent radicals based on

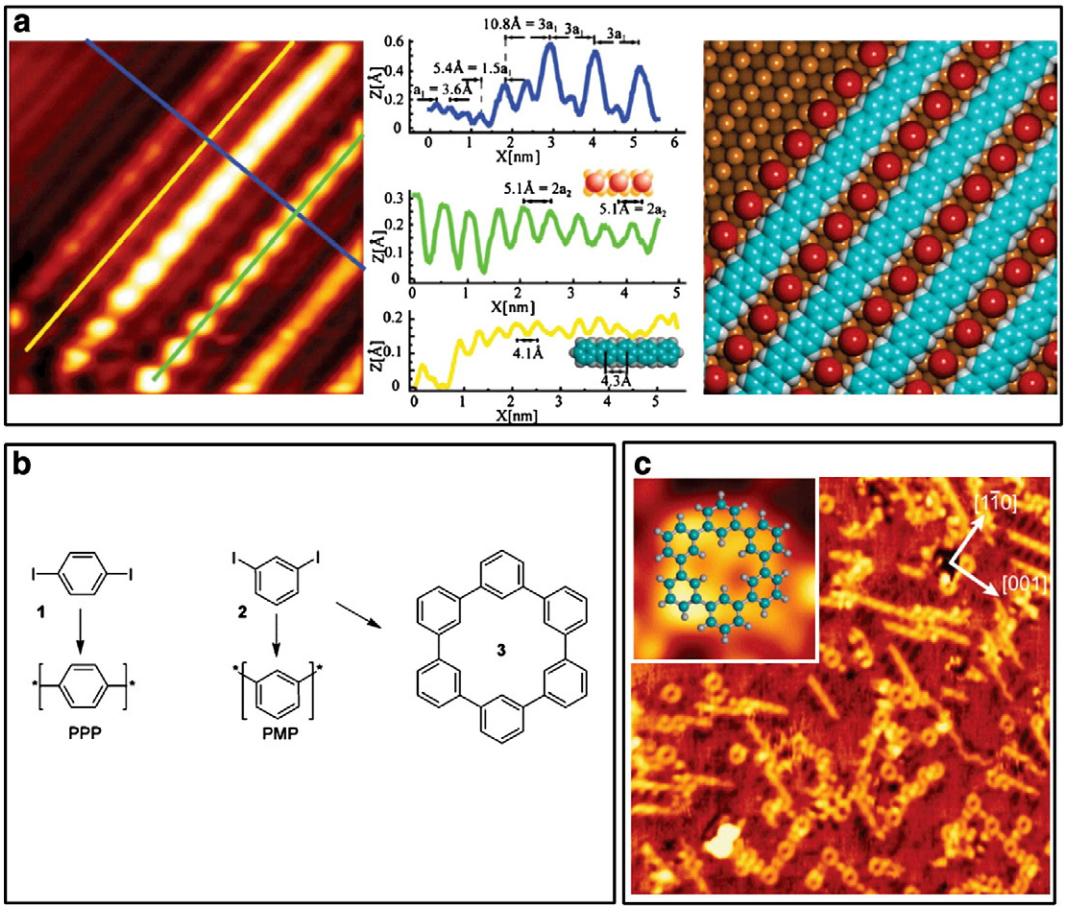


**Fig. 1.** a) STM image of 1,4-diiodobenzene lines formed after annealing at 500 K on Cu(110), the line profiles indicated the registry of the lines with respect to the substrate furrows (blue line), the spacing of the bright features (green profile), and the spacing of the dim lines (yellow profile). At the right is a model corresponding to the STM image. b) Scheme of the Ullmann coupling reaction. c) STM image of PMP oligomers scanned at 102 K; inset: a high resolution image of macrocycle. Figure reproduced from [30] with permission from Wiley-VCH Verlag GmbH & Co. KGaA, Weinheim.

the short distance between them [30,54]. Lin et al. recently supported this interpretation by revealing the signature of Cu atoms, which link two close radicals, using a combined STM/scanning tunneling spectroscopy (STS) study and DFT calculations [55].

### 2.4. Polymerization of carbenes and alkanes

Polymerization at the surface can also be achieved using carbene molecules, as demonstrated by Matena et al. using 1,3,8,10-tetraazaperopyrene (TAPP) molecule to form polymer "lines" on Cu(111) [56,57]. The deposition of TAPP on Cu(111) at ambient conditions followed by annealing at 450 K (or deposition directly onto a surface held at the same temperature) leads to the formation of porous networks based on metal-organic coordination. After annealing the sample at 550 K, a polymeric chain was formed [57]. Matena et al. employed XPS study to characterize the chemical nature of different structures observed on the surface (metal–organic and polymer). They based their measurements on the nitrogen atom because it possesses a different chemical environment between coordination network and polymeric structure. The coordination network is characterized by one N1s peak at 398.74 eV, whereas the polymeric chain exhibits and additional peak at 398.10 eV [57].

The formation of C – C bonds has also been achieved between linear chains of alkanes. Zhong et al. demonstrated that the Au(110) surface serves as both template and catalyst for alkyl C – H activation [58]. The polymerization was the result of both the surface topography of the Au(110) surface and C – H bond activation. Annealing the sample at 440 K for 30 min produces a phase transition from a $(1 \times 2)$ to a $(1 \times 3)$ reconstruction, where the grooves formed have a 1.22 nm periodicity. The diffusion of the alkanes is confined by the atomic grooves of the $(1 \times 3)$ phase, forcing the molecules into a 1D structure. Next, C – H bond activation occurs from the end of the molecular chains accompanied by desorption of hydrogen atoms. Consequently, C – C bond formation takes place, resulting in the creation of a polymer 1D. The authors demonstrate that the molecular chains can be pulled out of the grooves using STM tip manipulation, confirming that the structures are covalently bonded. In addition, the authors also performed an STM study using another molecule (1,4-di(eicosyl)benzene) [58] to confirm the dehydrogenative polymerization reaction.

## 3. Two-dimensional surface-confined polymerization

### *3.1. Polymer formation mechanisms*

The first surface-synthesized 2D covalently-bound molecular nanostructures were reported by Grill et al. in 2007 [19]. The authors demonstrated that the topology of these nanostructures can be engineered by controlling the geometry of the reactive sites on the monomer. They used porphyrin monomers with different numbers and positions of bromine atoms. Two methodologies were adopted to create these nanostructures: the first was to deposit the molecule on Au(111) at room temperature and subsequently anneal the system to cleave the halogen, and the second was achieved by heating the porphyrin monomer in the effusion cell to liberate the bromine atoms, depositing the dehalogenated molecules directly on the surface with no subsequent annealing. To demonstrate the covalent bonding in the

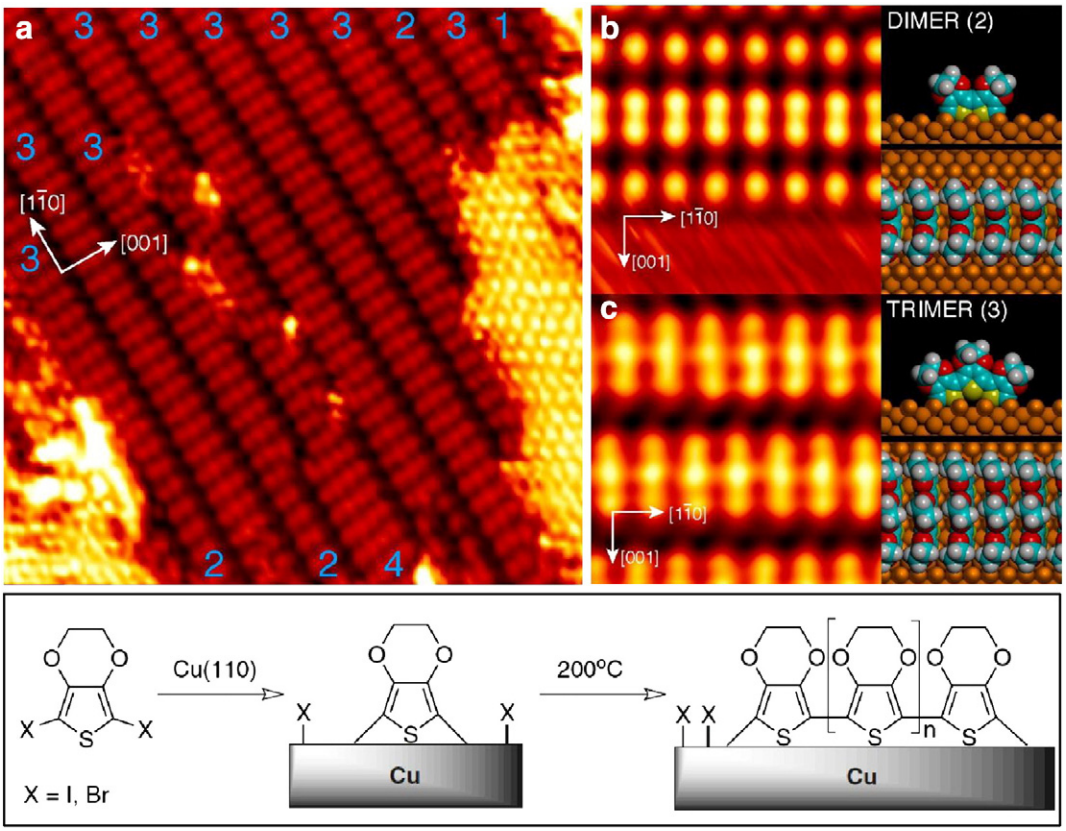


**Fig. 2.** a) STM image of surface covered with DIEDOT oligomers, revealing fusing of the DIEDOT elements. Monomers (1), dimers (2), trimers (3), and tetramers (4) are identified, surrounded by a (brighter) region of species in a c(2 × 2) reconstruction. b) and c) High resolution STM images with DFT calculated model of the dimer and trimer, respectively. Figure reproduced from [31] with permission from Proceeding of the National Academy of Science of the United States of Americas.

structures, Grill et al. manipulated the polymerized molecules using the STM tip to emphasize the robust character of the bonding. In addition, they showed that the periodicity measured between two adjacent polymerized porphyrins is in agreement with DFT simulations.

Using a two-step reaction, Cai et al. demonstrated the fabrication of graphene nanoribbons (GNRs) (Fig. 3) [20]. Experiments were performed using different monomers on the Au(111) and Ag(111) surfaces. The formation of armchair ribbons was achieved by the deposition of monomers **1** and **2** (Fig. 3a, c) onto a surface held at 500 K and 550 K respectively to induce a dehalogenation process and radicals addition. Next, systems **1** and **2** were annealed respectively to 700 K and 740 K, so that cyclo-dehydrogenation took place. To confirm these reactions and exemplify the quality of GNRs, the authors used additional techniques including XPS and Raman to quantify, respectively, the quality and the width of the GNRs. Thus, as shown in Fig. 3e, the sharp peak at 396 $cm^{-1}$ exhibits what is called width-specific radial-breathing-like mode demonstrating experimentally that the radial-breathing-like mode is highly sensitive for probing the GNRs. XPS spectra acquired after the polymerization of monomer **2** indicate only the presence of C1s at 284.5 eV (Fig. 3f) and the presence of other components such as C–O, C═O or COOH was not observed which means that GNRs are chemically pure and inert under ambient conditions.

Recently, Grill et al. demonstrated that the use of selective and sequential activation of specific sites on the monomer to facilitate hierarchical 2D polymer growth [59]. A porphyrin molecule with two different types of halogen (bromine and iodine) in the trans configuration was used as monomer building block (Fig. 4a). The isolated monomer was identified in STM images by its square shape, attributed to the porphyrin block, with two sets of diametrically opposed protrusions of different brightness. The authors attribute the brighter ones to the iodine atoms and the darker to the bromine atoms (Fig. 4b). To control the sequential activation, Grill et al. deposited the monomer on Au(111) held at 80 K, which preserved the molecules intact on the surface (Fig. 4b). Heating the system to 420 K led to the selective dissociation of the iodine atoms, while leaving the bromine atoms attached to the monomers, and consequently to the formation of a 1D polymer structure (Fig. 4c). The formation of 2D polymer networks was subsequently achieved by annealing the system to 550 K (Fig. 4d). The authors describe this in terms of the dissociation of the bromine atoms from the 1D chains and the subsequent diffusion to form C–C interchain bonds. The mobility of the 1D polymer structure was verified by an STM study. To demonstrate control of the geometry and composition of the covalent system, the authors deposited both trans-$Br_2I_2$TPP and dibromoterfluorene (DBTF) on Au(111) and heated the system up to 550 K. The two-step polymerization reaction was achieved first by forming 1D chains of TPP blocks upon cleaving iodine atoms and secondly by connecting the DBTF monomers to the 1D polymer of TPP after the dissociation of the bromine atoms.

Other experiments have also demonstrated a step-wise reaction approach to the fabrication of 2D polymer networks [60]. For example, using a dimethylmethylene-bridged triphenylamine (DTPA) precursor, Bieri et al. demonstrated the formation of a commensurate Ag(111) metal-coordination system after annealing to 500 K. Further heating the system to 600 K led to the formation of covalently bonded networks.

Condensation reactions [36–38] provide another route to on-surface 2D polymerization synthesis. These reactions were characterized by STM under UHV conditions, to identify the shape and size of the products. For this type of reaction a small molecule, like $H_2O$, is produced during molecule-molecule coupling. For example, Linderoth et al. reported the formation of imines as a result of polymerization reaction between aldehydes and amine molecules through a condensation reaction [36,38].

Boronic acid has also been successfully used to synthesize a surface-confined covalent network. The 2D polymer was formed starting from

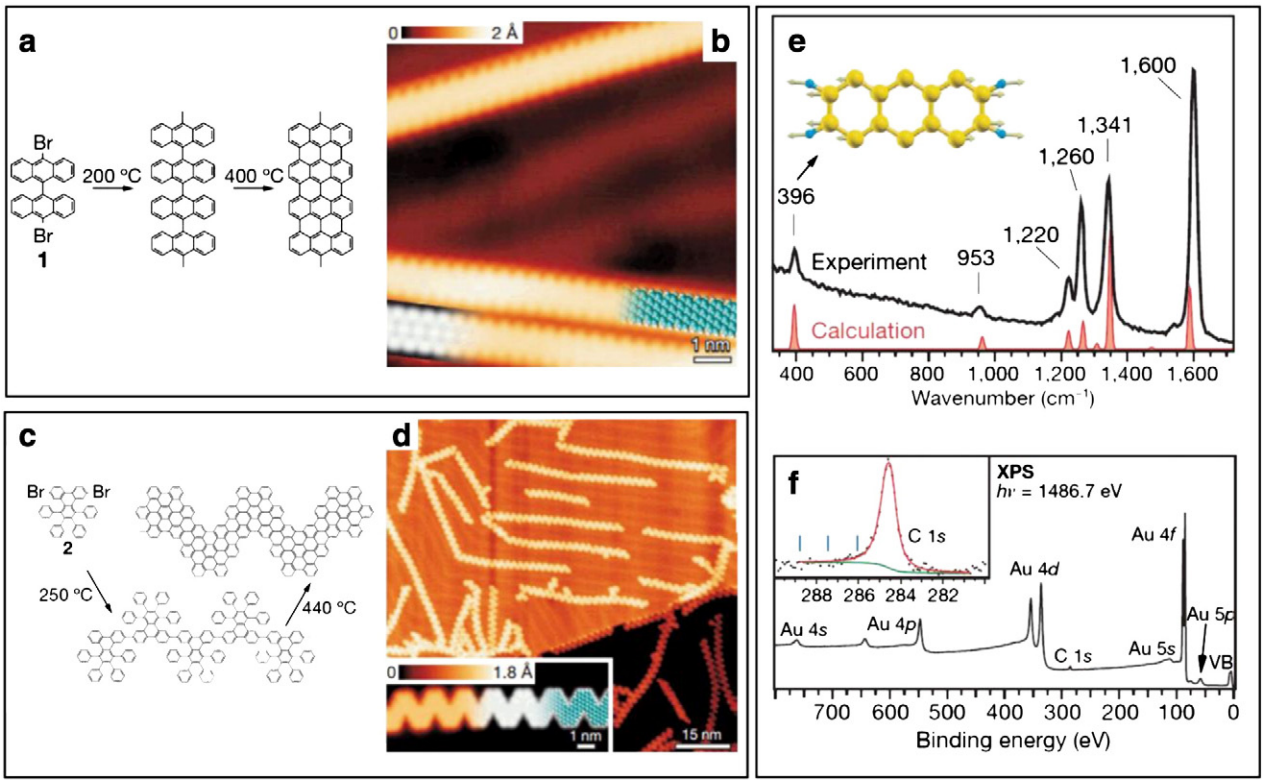


**Fig. 3.** a) Reaction scheme from precursor 1 to N = 7 armchair GNRs, b) STM image of polymer from monomer 1. c) Reaction scheme from precursor 2 to chevron-type GNRs. d) STM image polymer from monomer 2. e) Raman spectrum (532 nm) of N = 7 armchair GNRs. The inset shows the atomic displacements characteristic for the radial-breathing-like mode at 396 $cm^{-1}$. f) XPS survey of a monolayer sample of chevron-type GNRs with core levels and valence band. (Inset) C1s XPS spectra. Figure reproduced from [20] with permission from Nature Publishing Group.

1,4-benzenediboronic acid (BDBA) building blocks. The experimental results reported by Zwaneveld et al. show that BDBA molecules form a hexagonal network on Ag(111), and that the porous structure remains stable and undamaged even following annealing to 750 K for 5 min (Fig. 5) [37]. In addition, by co-depositing BDBA and 2,3,6,7,10,11-hexahydroxytriphenylene (HHTP) the authors were able to control the pore size of the network. The co-adsorption of both BDBA and HHTP molecules on Ag(111) leads to the formation of a porous hexagonal structure where the diameter of the nanopores is larger by 14.55 Å than in the network formed by BDBA alone.

Based on the boronic condensation as a polymerization reaction, Dienstmaier et al. demonstrated the formation of a long-range ordered

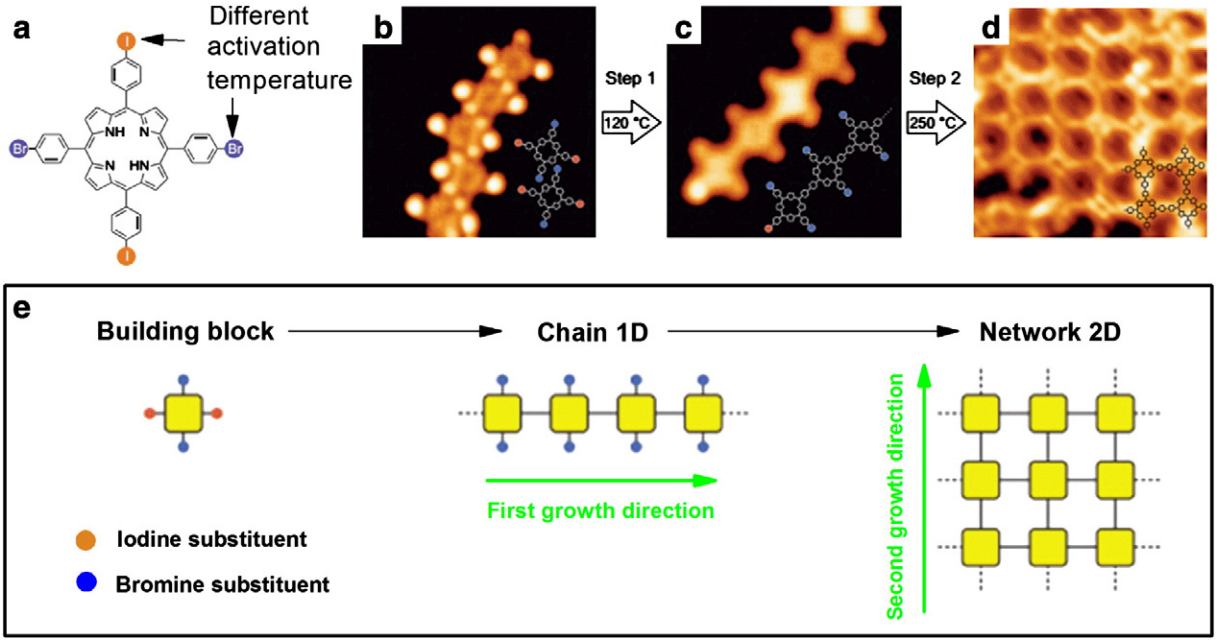


**Fig. 4.** a) Chemical structure of the trans-$Br_2I_2$TPP. b) STM image of trans-$Br_2I_2$TPP/Au(111) system at 80 K. c) Formation of 1D polymer chain. d) Formation of 2D polymer structure. e) Scheme of sequential activation mechanism. Figure reproduced from [59] with permission from Nature Chemistry.

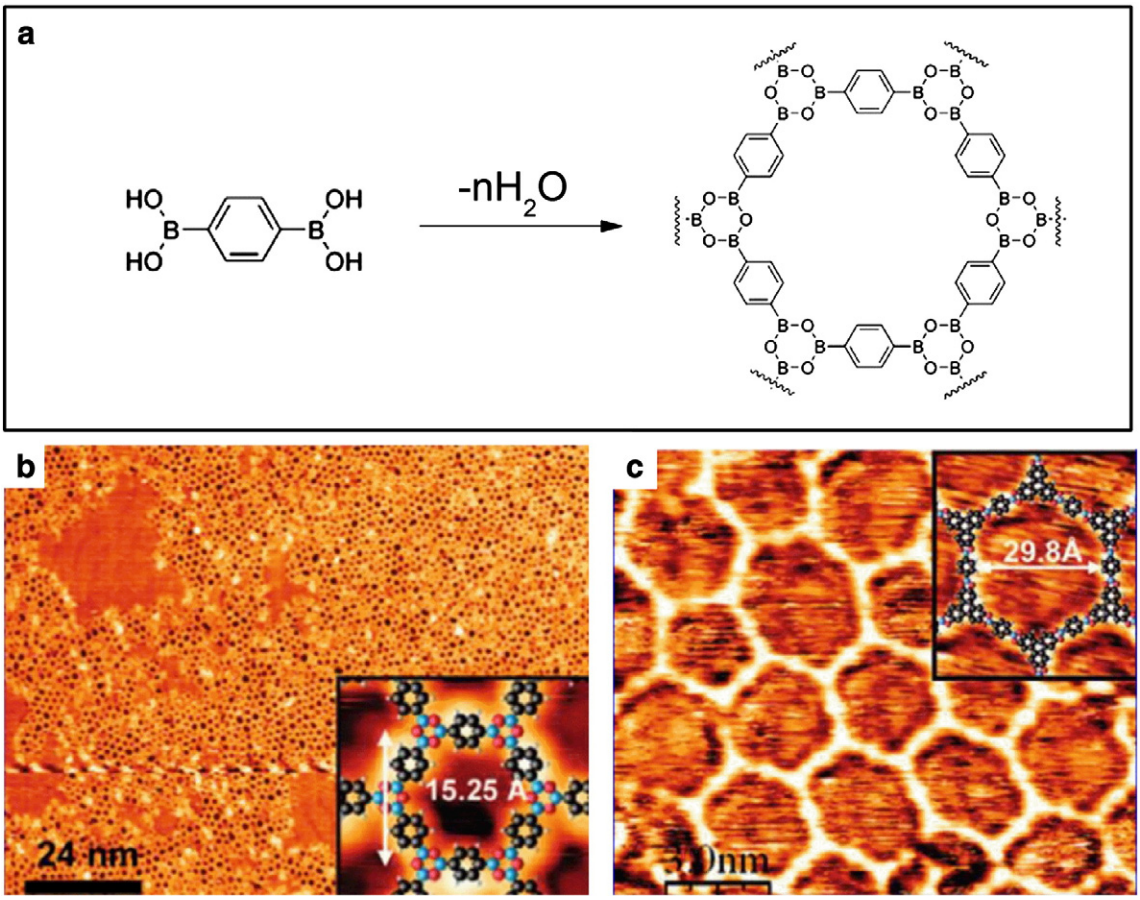


**Fig. 5.** a) Scheme of condensation polymerization reaction. b) STM images of 2D polymer networks of BDBA. c) BDBA and HHTP co-condensation. Inset a model of porous nanostructure of each system. Figure reproduced from [37] with permission from the American Chemical Society.

monolayer covalent organic framework (COF) [61]. They used two synthetic approaches. In the first the BDBA monomers are first prepolymerized via solvothermal synthesis [62] and then drop-cast on a graphite surface where they are characterized by STM. In the second approach, the condensation reaction was thermally activated after deposition of the BDBA-containing solvent. A similar study was presented by Guan et al. based on a reversible condensation polymerization reaction were the $H_2O$ produced during the coupling reaction of monomers can be reintroduced to reverse the reaction and correct defects within the networks [63]. Heating the biphenyldiboronic acid-HOPG system leads to the condensation polymerization reaction, whereas the presence of a small amount of water can reverse the mechanism to form the initial monomers on the surface. The last experiment demonstrates an example of polymerization reactions that are reversible on a surface. The reversibility of the mechanism was explained by heating and cooling the system with the presence of copper (II) sulfate pentahydrate where the $H_2O$ liberated from the latter, during heating, can act as an equilibrium-manipulating agent to favor the correction of defects.

Using a combined mechanism of condensation polymerization and Ullmann coupling, Faury et al. reported the formation of a COF on the Au(111) surface under UHV conditions [64]. A bi-functional precursor, containing both bromine atom and boronic acid, was used. The latter reacts on Au(111) under thermal activation (400 K) to form trimers linked by a boroxine ring. These trimers were then annealed on the surface at 550 K to cleave the C–Br bond and consequently form the COF structure. The competing reactions provide a new way to synthesize 2D covalently networks. However, some limitations such as disorder in the structure of the COF remain to be addressed.

### 3.2. The role of the surface

While the methodologies described above relied predominantly on the chemical nature of the monomers to create 2D networks, Gutzler et al. and Bieri et al. have investigated the effect of different surfaces on the formation of 2D polymers. Gutzler et al. studied brominated monomers (1,3,5-tris(4-bromophenyl)benzene, TBPB) on Cu(111) and Ag(110) to synthesize COFs. These substrates were used to elucidate the energetic role of the surface in the dissociation of C-Br bond. Following the deposition of TBPB molecules on Cu(111) held at ~80 K, the formation of a self-assembled pattern stabilized by halogen-halogen interactions occurs [33]. At 300 K dissociation of C-Br bonds occurs, and consequently organo-metallic complex is formed. However, under the same conditions no debromination of TBPB was observed on Ag(111) or Au(111) substrates [54]. Based on a measurement of the reduced distance between the debrominated molecules, Gutzler et al. demonstrated the synthesis of a nanoporous polymeric structure achieved by annealing the TBPB/Cu(111) system at 500 K. To form covalent bonds on these different surfaces additional thermal activation is imposed to link the radicals. The activation barrier varies from substrate to substrate, and this needs to be accounted for in the preparation of the polymer, as discussed further below.

Bieri et al. demonstrated the importance of substrate reactivity through a series of experiments employing the precursor hexaiodo-substituted macrocycle cyclohexa-m-phenylene (CHP) on three different substrates: Ag(111), Au(111), and Cu(111) [39]. Single crystal noble metals are characterized by composition- and facet-dependent structural and electronic properties. For these fcc crystals, (111) facets are

closer packed than either the (100) or (110) facets. (111) facets offer three possible adsorption sites: on-top, bridge (between two atoms) and hollow (between three atoms). However, (110) facets provide a number of sites such as on-top, short-bridge, long-bridge and hollow-sites located between four atoms. The Cu(110) surface is characterized by two-fold symmetry i.e. rectangular atomic lattice, and is atomically rough and anisotropic. Ag(110) and Au(110) present similarly anisotropic diffusion landscapes, and Au(110) can have reconstructions with unit cells ranging from $1 \times 2$ to $1 \times 5$ [65]. The structural properties of the noble metal substrates affect the reactivity of the surfaces (effect of electronic property [65]), and consequently impact the intermolecular interactions leading to the formation of various molecular architectures. Bieri et al. studied two major factors, namely the reactivity and mobility of the (111) facets of Cu, Ag and Au (Fig. 6). Using a combination of STM and Monte Carlo simulations, the authors demonstrated that relative to the other surfaces, Cu(111) presents more reactive sites and a reduced mobility of the adsorbed molecules. The difference between the same facet of different noble metals can be seen, for example, for pentacene, where a type of hybridization has been proposed for pentacene/Cu(111) and pentacene/Ag(111) [66], whereas the interaction of pentacene with Au(111) is weaker. In a study of different low-index Cu facets, Tautz reported that PTCDA molecules chemisorbed on (111), (110) and (100) [67]. Taken together, these studies emphasize the strong reactivity of Cu, especially when compared to Au. In fact, Au(111) is often specifically employed when a weak interaction between the molecule and the surface is desired (e.g. for pentacene [66]). The Au(111) surface provides an almost uniform reserve of electronic charges. As shown in Fig. 6C and D, CHP molecules were observed to form a mixture of branched and dense structure on Au(111) after annealing at 745 K demonstrating the weak interaction of the surface/molecule couple. On the other hand, Ag(111) exhibits properties between those of Cu(111) and Au(111). As shown in Figs. 6E and F, Ag(111) is characterized by reactivity and mobility proprieties opposite to those of Cu(111) [39].

To date, polymerization reactions for the formation of 1D and 2D conjugated structures have been primarily studied on conducting substrates. However, initial work shows that these polymers networks can be formed on nonmetallic surfaces as well. Recent work has shown that on calcite, the electrostatic interactions between the carboxylate groups of halide-substituted benzoic acid and the surface of calcium action can be employed to prevent desorption and allow hemolytic cleaving of the molecule due to a temperature effect [68]. The formation of the phtalocyanine has been achieved onto a thin insulating film [69] by the simultaneous deposition of 1,2,4,5-tetracyanobenzene and iron atoms. These studies demonstrate the possibility for utilizing dielectric surfaces as supports for the synthesis of conjugated polymers and provide an important step towards exploiting these polymers in molecular electronics.

Finally, we note that the choice of the environment has important implications for the polymerization recation. In particular, the methods available to initiate polymerization differ between solution and vacuum. At the liquid-solid interface, polyermization has been achieved by voltage pluses [44], UV irradaiation and electrochemical techniques [43]. Under UHV conditions STM tip pulses [51], thermal and surface catalytic effects [19,20,30,33] and condensation reactions [37] have been used to invoke polymerization reactions. The challenge of scaling 2D surface-confined polymerization to production scale, in anticipation of device applications, may require more careful exploration of solution-processed routes, such as the drop-deposition method by which Russell et al demonstrated dimeric coupling of tri (4-bromophenyl) benzene [70].

## 4. Conclusion and perspectives

Lines and sheets with varying spatial extents have been successfully formed from molecules covalently bonded through various coupling reactions. Although the covalent structures have predominantly been characterized by scanning probe methods to date, a variety of surface

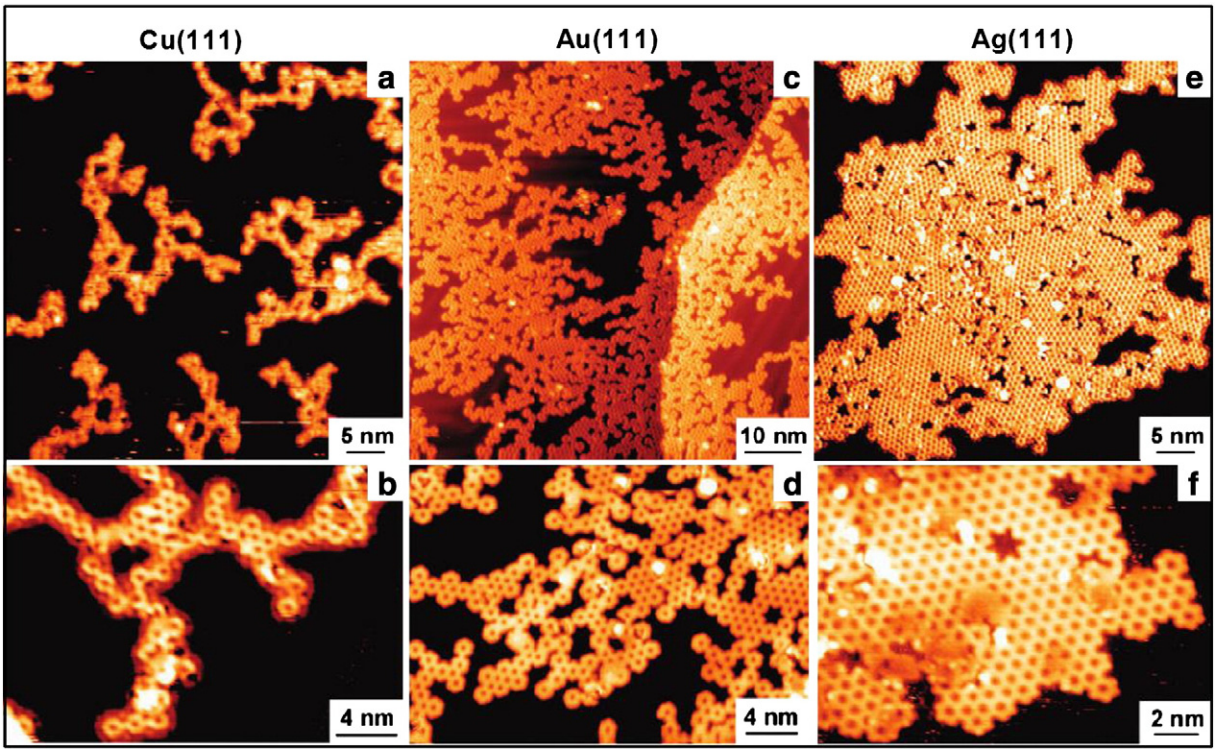


**Fig. 6.** STM of polymerized structure resulting from the precursor hexaiodo-substituted macrocycle cyclohexa-m-phenylene (CHP) on three different surfaces, Cu(111), Ag(111) and Au(111), showing large- (A, C, E) and small-scale (B, D, F) structure within the networks. Figure reproduced from [39] with permission from American Chemical Society.

science techniques can also offer the possibility to analyze both their structural and electronic proprieties. The applications potential for this type of system has been demonstrated by their robustness and stability on the surface, although direct measurements of their electronic proprieties remain to be made. Presently, the largest technical challenge lies in improving the perfection of the molecular networks.

This challenge is the objective of various studies that focused specifically on the molecule/substrate pair, a key factor in tailoring the characteristics of epitaxial growth. Recent work has focused on the study of different surface properties, namely atomic structure, active sites on the surface and changes in reactivity between different facets (e.g. the low-index facets of fcc crystals). The reactivity of a facet depends strongly on its electronic properties, which are critically dependent on the orientation of the surface. An intensive effort must be made to understand the effect of atomic structure and electronic properties on intermolecular reactions and consequently on the polymerization process.

The surface mobility of molecules is influenced by the nature of the surface, notably the diffusion barrier, which changes from one substrate to another [39]. The morphology and atomic structure of the surface can also have an impact on molecular growth. The presence of different active sites such as steps, kink and step-edges also play an important role in the reaction mechanism [71]. On the other hand, the use of monomers with multiple polymerization sites could provide another way to "control" the mechanism of the polymerization reaction at the surface [59].

To date, various building blocks have been used to achieve a range of different surface-confined molecular structures. For example, radical addition has demonstrated its potential to create 0D, 1D, and 2D covalent structures with the ability to correct topological defects. This approach requires the use of catalytic substrates to create the radicals that can lead to on-surface polymerization. Then, thermal energy is used to produce a modification in the structure from molecular self-assembly to polymerization. However, work remains to be done to understand the mechanism of the reaction. Understanding the effects of intrinsic substrate properties is a crucial step for controlling the reaction at the surface. For example, free substrate adatoms are a non-negligible part of the reaction. Understanding their positions within the atomic structure of the surface and their temperature-dependent behaviors are important first steps.

The synthesis of new materials through on-surface reactions offers the possibility to fabricate robust structures that exhibit excellent thermal stability with the possibility to control characteristic features sizes, for example, pore size. This represents an important step towards controlling the growth of these materials and integrating them into molecular electronic devices. The next steps will be achieved by improving their structural properties and by measuring and optimizing their electron transport, especially in 2D conjugated polymer networks, to move them closer to applications in sensors and devices.

## Acknowledgments

This work was supported by the Natural Sciences and Engineering Research Council of Canada (NSERC) through a Discovery Grant, the Fonds Quebecois sur la Recherche en Nature et Technologies (FQRNT) through a Team Grant and the Ministere du Developpement Economique de l'Innovation et de l'Exportation (MDEIE) through an international collaboration Grant. Federico Rosei is grateful to the Canada Research Chairs program for partial salary support and to the Alexander von Humboldt Foundation for a FW Bessel Award.

## References

[1] J.E. Green, J.W. Choi, A. Boukai, Y. Bunimovich, E. Johnston-Halperin, E. Delonno, Y. Luo, B.A. Sheriff, K. Xu, Y.S. Shin, H.R. Tseng, J.F. Stoddart, J.R. Heath, Nature 445 (2007) 414.
[2] M. El Garah, F. Palmino, F. Cherioux, Langmuir 26 (2010) 943.
[3] F. Rosei, M. Schunack, Y. Naitoh, P. Jiang, A. Gourdon, E. Laegsgaard, I. Stensgaard, C. Joachim, F. Besenbacher, Prog. Surf. Sci. 71 (2003) 95.
[4] J.M. MacLeod, O. Ivasenko, C.Y. Fu, T. Taerum, F. Rosei, D.F. Perepichka, J. Am. Chem. Soc. 131 (2009) 16844.
[5] J.V. Barth, J. Weckesser, G. Trimarchi, M. Vladimirova, A. De Vita, C.Z. Cai, H. Brune, P. Gunter, K. Kern, J. Am. Chem. Soc. 124 (2002) 7991.
[6] M.E. Canas-Ventura, W. Xiao, D. Wasserfallen, K. Mullen, H. Brune, J.V. Barth, R. Fasel, Angew. Chem. Int. Edit. 46 (2007) 1814.
[7] K.G. Nath, O. Ivasenko, J.M. MacLeod, J.A. Miwa, J.D. Wuest, A. Nanci, D.F. Perepichka, F. Rosei, J. Phys. Chem. C 111 (2007) 16996.
[8] C.A. Palma, P. Samori, Nat. Chem. 3 (2011) 431.
[9] O. Ivasenko, J.M. MacLeod, K.Y. Chernichenko, E.S. Balenkova, R.V. Shpanchenko, V.G. Nenajdenko, F. Rosei, D.F. Perepichka, Chem. Commun. (2009) 1192.
[10] S. De Feyter, A. Miura, S. Yao, Z. Chen, F. Wurthner, P. Jonkheijm, A.P.H.J. Schenning, E.W. Meijer, F.C. De Schryver, Nano Lett. 5 (2005) 77.
[11] R. Gutzler, O. Ivasenko, C.Y. Fu, J.L. Brusso, F. Rosei, D.F. Perepichka, Chem. Commun. 47 (2011) 9453.
[12] K.H. Chung, J. Park, K.Y. Kim, J.K. Yoon, H. Kim, S. Han, S.J. Kahng, Chem. Commun. 47 (2011) 11492.
[13] R. Gutzler, C.Y. Fu, A. Dadvand, Y. Hua, J.M. MacLeod, F. Rosei, D.F. Perepichka, Nanoscale 4 (2012) 5965.
[14] R. Decker, U. Schlickum, F. Klappenberger, G. Zoppellaro, S. Klyatskaya, M. Ruben, J.V. Barth, H. Brune, Appl. Phys. Lett. 93 (2008) 243102.
[15] M. Marschall, J. Reichert, A. Weber-Bargioni, K. Seufert, W. Auwarter, S. Klyatskaya, G. Zoppellaro, M. Ruben, J.V. Barth, Nat. Chem. 2 (2010) 131.
[16] U. Schlickum, R. Decker, F. Klappenberger, G. Zoppellaro, S. Klyatskaya, M. Ruben, I. Silanes, A. Arnau, K. Kern, H. Brune, J.V. Barth, Nano Lett. 7 (2007) 3813.
[17] N.R. Champness, Nat. Nanotechnol. 2 (2007) 671.
[18] A. Gourdon, Angew. Chem. Int. Edit. 47 (2008) 6950.
[19] L. Grill, M. Dyer, L. Lafferentz, M. Persson, M.V. Peters, S. Hecht, Nat. Nanotechnol. 2 (2007) 687.
[20] J.M. Cai, P. Ruffieux, R. Jaafar, M. Bieri, T. Braun, S. Blankenburg, M. Muoth, A.P. Seitsonen, M. Saleh, X.L. Feng, K. Mullen, R. Fasel, Nature 466 (2010) 470.
[21] D.F. Perepichka, F. Rosei, Science 323 (2009) 216.
[22] A.J. Heeger, Rev. Mod. Phys. 73 (2001) 681.
[23] M. Granstrom, K. Petritsch, A.C. Arias, A. Lux, M.R. Andersson, R.H. Friend, Nature 395 (1998) 257.
[24] J.H. Burroughes, D.D.C. Bradley, A.R. Brown, R.N. Marks, K. Mackay, R.H. Friend, P.L. Burns, A.B. Holmes, Nature 347 (1990) 539.
[25] S.R. Forrest, Nature 428 (2004) 911.
[26] A. Dadvand, A.G. Moiseev, K. Sawabe, W.H. Sun, B. Djukic, I. Chung, T. Takenobu, F. Rosei, D.F. Perepichka, Angew. Chem. Int. Edit. 51 (2012) 3837.
[27] M. Muccini, Nat. Mater. 5 (2006) 605.
[28] G. Horowitz, Adv. Mater. 10 (1998) 365.
[29] C.D. Dimitrakopoulos, P.R.L. Malenfant, Adv. Mater. 14 (2002) 99.
[30] J.A. Lipton-Duffin, O. Ivasenko, D.F. Perepichka, F. Rosei, Small 5 (2009) 592.
[31] J.A. Lipton-Duffin, J.A. Miwa, M. Kondratenko, F. Cicoira, B.G. Sumpter, V. Meunier, D.F. Perepichka, F. Rosei, Proc. Natl. Acad. Sci. U.S.A. 107 (2010) 11200.
[32] M.O. Blunt, J.C. Russell, N.R. Champness, P.H. Beton, Chem. Commun. 46 (2010) 7157.
[33] R. Gutzler, H. Walch, G. Eder, S. Kloft, W.M. Heckl, M. Lackinger, Chem. Commun. (2009) 4456.
[34] M. Treier, R. Fasel, N.R. Champness, S. Argent, N.V. Richardson, Phys. Chem. Chem. Phys. 11 (2009) 1209.
[35] M. Treier, N.V. Richardson, R. Fasel, J. Am. Chem. Soc. 130 (2008) 14054.
[36] S. Weigelt, C. Busse, C. Bombis, M.M. Knudsen, K.V. Gothelf, T. Strunskus, C. Woll, M. Dahlbom, B. Hammer, E. Laegsgaard, F. Besenbacher, T.R. Linderoth, Angew. Chem. Int. Edit. 46 (2007) 9227.
[37] N.A.A. Zwaneveld, R. Pawlak, M. Abel, D. Catalin, D. Gigmes, D. Bertin, L. Porte, J. Am. Chem. Soc. 130 (2008) 6678.
[38] S. Weigelt, C. Busse, C. Bombis, M.M. Knudsen, K.V. Gothelf, E. Laegsgaard, F. Besenbacher, T.R. Linderoth, Angew. Chem. Int. Edit. 47 (2008) 4406.
[39] M. Bieri, M.T. Nguyen, O. Groning, J.M. Cai, M. Treier, K. Ait-Mansour, P. Ruffieux, C.A. Pignedoli, D. Passerone, M. Kastler, K. Mullen, R. Fasel, J. Am. Chem. Soc. 132 (2010) 16669.
[40] W. Ho, J. Chem. Phys. 117 (2002) 11033.
[41] C. Joachim, J.K. Gimzewski, IEEE 86 (1998) 184.
[42] M. Magoga, C. Joachim, Phys. Rev. B 56 (1997) 4722.
[43] P.C.M. Grim, S. De Feyter, A. Gesquiere, P. Vanoppen, M. Rucker, S. Valiyaveettil, G. Moessner, K. Mullen, F.C. De Schryver, Angew. Chem. Int. Edit. 36 (1997) 2601.
[44] Y. Okawa, M. Aono, Nature 409 (2001) 683.
[45] Y. Okawa, M. Aono, J. Chem. Phys. 115 (2001) 2317.
[46] Y. Okawa, M. Aono, J. Surf. Sci. Nanotechnol. 2 (2004) 99.
[47] S.P. Sullivan, A. Schmeders, S.K. Mbugua, T.P. Beebe, Langmuir 21 (2005) 1322.
[48] H. Sakaguchi, H. Matsumura, H. Gong, Nat. Mater. 3 (2004) 551.
[49] H. Sakaguchi, H. Matsumura, H. Gong, A.M. Abouelwafa, Science 310 (2005) 1002.
[50] F. Ullmann, J. Bielecki, Ber. Dtsch. Chem. Ges. 34 (1901) 2174.
[51] S.-W. Hla, L. Bartels, G. Meyer, K.-H. Rieder, Phys. Rev. Lett. 85 (2000) 2777.
[52] G.S. McCarty, P.S. Weiss, J. Am. Chem. Soc. 126 (2004) 16772.
[53] M.M. Blake, S.U. Nanayakkara, S.A. Claridge, L.C. Fernandez-Torres, E.C.H. Sykes, P.S. Weiss, J. Phys. Chem. A 113 (2009) 13167.
[54] H. Walch, R. Gutzler, T. Sirtl, G. Eder, M. Lackinger, J. Phys. Chem. C 114 (2010) 12604.
[55] W.H. Wang, X.Q. Shi, S.Y. Wang, M.A. Van Hove, N. Lin, J. Am. Chem. Soc. 133 (2011) 13264.

[56] M. Matena, M. Stohr, T. Riehm, J. Bjork, S. Martens, M.S. Dyer, M. Persson, J. Lobo-Checa, K. Muller, M. Enache, H. Wadepohl, J. Zegenhagen, T.A. Jung, L.H. Gade, Chem. Eur. J. 16 (2010) 2079.
[57] M. Matena, T. Riehm, M. Stohr, T.A. Jung, L.H. Gade, Angew. Chem. Int. Edit. 47 (2008) 2414.
[58] D.Y. Zhong, J.H. Franke, S.K. Podiyanachari, T. Blomker, H.M. Zhang, G. Kehr, G. Erker, H. Fuchs, L.F. Chi, Science 334 (2011) 213.
[59] L. Lafferentz, V. Eberhardt, C. Dri, C. Africh, G. Comelli, F. Esch, S. Hecht, L. Grill, Nat. Chem. 4 (2012) 215.
[60] M. Bieri, S. Blankenburg, M. Kivala, C.A. Pignedoli, P. Ruffieux, K. Mullen, R. Fasel, Chem. Commun. 47 (2011) 10239.
[61] J.F. Dienstmaier, A.M. Gigler, A.J. Goetz, P. Knochel, T. Bein, A. Lyapin, S. Reichlmaier, W.M. Heckl, M. Lackinger, ACS Nano 5 (2011) 9737.
[62] A.P. Cote, A.I. Benin, N.W. Ockwig, M. O'Keeffe, A.J. Matzger, O.M. Yaghi, Science 310 (2005) 1166.
[63] C.Z. Guan, D. Wang, L.J. Wan, Chem. Commun. 48 (2012) 2943.
[64] T. Faury, S. Clair, M. Abel, F. Dumur, D. Gigmes, L. Porte, J. Phys. Chem. C 116 (2012) 4819.
[65] M. Pedio, C. Cepek, R. Felici, Organic molecules on noble metal surfaces: the role of the interface, in: Dr. Yen-Hsun Su (Ed.), Noble Metals, InTech, ISBN: 978-953-307-898-4, 2012, http://dx.doi.org/10.5772/34551, (Available from: http://www.intechopen.com/books/noblemetals/organicmolecules-on-noble-metal-surfaces-the-role-of-the-interface).
[66] B. Jaeckel, J.B. Sambur, B.A. Parkinson, J. Appl. Phys. 103 (2008) 063719.
[67] F.S. Tautz, Prog. Surf. Sci. 82 (2007) 479.
[68] M. Kittelmann, P. Rahe, A. Gourdon, A. Kühnle, ACS Nano 6 (2012) 7406.
[69] M. Abel, S. Clair, O. Ourdjini, M. Mossoyan, L. Porte, J. Am. Chem. Soc. 133 (2010) 1203.
[70] J.C. Russell, M.O. Blunt, J.M. Garfitt, D.J. Scurr, M. Alexander, N.R. Champness, P.H. Beton, J. Am. Chem. Soc. 133 (2011) 4220.
[71] A. Saywell, J. Schwarz, S. Hecht, L. Grill, Angew. Chem. Int. Edit. 51 (2012) 5096.